
# LOCATION AWARENESS VIA INTELLIGENT SURFACES

## *A Path Toward Holographic NLN*

Moe Z. Win, Ziyi Wang, Zhenyu Liu, Yuan Shen, and Andrea Conti

Location information is critical for numerous applications, such as smart cities, autonomous vehicles, and Industry 4.0. In this article, we present the paradigm of holographic network localization and navigation (NLN), namely NLN with holographic radios. We describe holographic NLN enabled by reconfigurable intelligent surfaces (RISs), where the phase responses of the RISs are controlled to create desirable electromagnetic (EM) environments for wireless communications. Specifically, we present a mathematical model for signal transmission and reception in the presence of RISs. This model applies to both continuous intelligent surfaces (CISs) and discrete intelligent surfaces (DISs) and accounts for the polarization and directivity of antennas. We review recent research progress on RISs and summarize their characteristics that benefit communication and localization. We present key ingredients of NLN and describe how RISs can be employed to enable holographic NLN. We quantify the performance of RIS-enabled

*Digital Object Identifier 10.1109/MVT.2022.3157067*
*Date of current version: 24 May 2022*

***Location information is critical for numerous applications, such as smart cities, autonomous vehicles, and Industry 4.0.***

holographic NLN with a case study, showing that RISs can significantly improve localization accuracy, especially in scenarios where line-of-sight (LOS) paths between agents and anchors are obstructed.

## Overview

Location awareness is essential for a variety of location-based services (LBSs). For most outdoor scenarios, position information can be provided by global navigation satellite systems. However, in harsh and complicated wireless propagation environments, such as indoor environments, new infrastructures and techniques are needed to fulfill the stringent requirements of LBSs.

In recent years, several techniques for high-accuracy localization in complicated wireless environments have been proposed, including the paradigm of NLN [1]. Existing works focus mainly on the design of localization techniques that are resilient and robust in wireless environments affected by multipath effect, cluttering, and non-line-of-sight (NLOS) propagation. The emerging intelligent surfaces (ISs) technology, which is a potential candidate for next-generation communication, provides an opportunity to control the EM environment [2]–[4]. ISs can be employed to create favorable wireless propagation conditions for localization [5], thus improving the performance limits of NLN [6]. In particular, nearly passive ISs, also known as RISs, are an important category of ISs. RISs consist of passive surfaces, active controllers, and sensing units, and they are typically known for low cost and low power consumption [7], [8].

In this article, we propose holographic NLN, i.e., NLN involving spatial spectral holography and spatial wave field synthesis. Holographic NLN is a new paradigm for controlling the EM environment to provide location awareness in challenging environments. Particularly, we focus on holographic NLN aided by RISs. Key questions related to RIS-enabled holographic NLN include:

- How does the structure of an RIS affect the EM environment for wireless localization?
- How can RISs benefit the performance of NLN, and what benefit do they provide?

The goal of this article is to present the fundamentals of RISs and show how they can be integrated into the paradigm of NLN to provide improved localization performance. We advocate the use of RISs to create a desirable EM environment for localization. The key idea is to direct the signals toward desired receivers and improve the quality of wireless measurements by controlling the phase response of RISs. With the assistance of RISs, the potential of NLN will be further unleashed, and new LBSs and applications will be enabled.

This article first reviews recent research progress on RISs and NLN and proposes a paradigm of holographic NLN. Then, we present CIS and DIS together with their associated signal models. These models enable the evaluation of the effect of the RIS element size in both near-field and far-field scenarios. Finally, this article introduces RIS-enabled holographic NLN and evaluates its performance in a case study. The case study shows that the proposed RIS configurations provide desirable localization performance and are robust in the presence of obstacles on scattering paths and direct paths.

## Holographic NLN

### *Reconfigurable Intelligent Surfaces*

RIS is the engineering embodiment of metasurfaces [7]. Metasurfaces are artificial structures synthesized by plenty of subwavelength elements, and their thickness is significantly less than the operating wavelength for which the metasurfaces are designed. Metasurfaces realize EM manipulation (phase, amplitude, and polarization), leading to applications such as wavefront shaping [9]. In 2011, phase-gradient metasurfaces and generalized Snell's laws were presented in [10]. Thin surfaces eliminate the volume constraints of bulky metamaterials. In 2012, metallic phase-gradient metasurfaces at microwave band as reflectarray were proposed, and the efficiency of such surfaces was close to 100% [11]. In these works, the phase-gradient metasurfaces were mainly fixed-structure metasurfaces, and the size of the microstructure on the surface was determined by the designed operating frequency.

In 2014, coding metamaterials were proposed in [12], which introduced reconfigurability into the phase-gradient metasurfaces. This property revealed the potential of metasurfaces in the field of information-processing systems. In 2018, phase-gradient metasurfaces, whose element size was smaller than half the operating wavelength, were proposed for the first time for imaging. Metasurfaces [13] with this property were viewed as continuous surfaces in the field of communications and localization [8]. In recent years, tunable phase-gradient metasurfaces have been investigated and fabricated for experimental verification [9].

Sensing units (e.g., active elements and RF chains) have been embedded in RISs to sense the environment autonomously. This allows RISs to adapt to the variation of the EM environment. Besides, RISs applied in wideband systems have also been also fabricated and investigated to expand their application in the areas of communication and localization.

### *Network Localization and Navigation*

NLN is a paradigm where networked nodes provide position information by performing measurements and communication in a collaborative manner [1]. This paradigm advocates the employment of spatiotemporal cooperation, soft information, and efficient network operation. In NLN, nodes with unknown positions are referred to as agents, while nodes with known positions are referred to as anchors. Anchors perform measurements to infer the agent's position. Navigation in NLN refers to tracking the positions of agents.

NLN is built on rigorous theoretical foundations [6] where the equivalent Fisher information matrix (EFIM) is employed to characterize the maximal amount of information about agent positions from measurements and prior knowledge [1]. Theoretical analyses provide the following insights:

1) Employing spatial cooperation remarkably benefits localization performance as measurements performed among agents also contribute to the EFIM.
2) Using signals with large bandwidth, such as ultra-wideband and millimeter-wave signals, improves the localization performance.
3) The obstruction of LOS paths can significantly degrade localization performance.
4) The geometric relationship between nodes is important to the localization performance.

Algorithms for inferring agent positions have been designed based on theoretical foundations [14]. These algorithms integrate different types of measurements and environmental knowledge with moderate computational effort. NLN also employs network operation algorithms for optimizing the topologies of the network and the allocation of communication resources in a holistic manner. Inference algorithms and network operation strategies for NLN have been validated via system implementation and network experimentation.

### *A Vision of Holographic NLN*

Holographic NLN is NLN involving spatial spectral holography and spatial wave field synthesis. RISs enable holographic NLN with improved accuracy, flexibility, and efficiency. In holographic NLN, a controlled EM environment is created by sensing the wireless environment and adjusting the phase responses of the RISs accordingly. Such control of the EM environment will create additional effective connections among agents and anchors in the network, improve the received signal-to-noise ratio (SNR), bridge indoor and outdoor environments, and enhance spatiotemporal cooperation in NLN. Compared with classical NLN, holographic NLN facilitates additional cooperation between RISs, agents, and anchors and leads to additional position information.

Figure 1 shows an example of holographic NLN, where the static base stations on the buildings correspond to anchors, and the vehicle, pedestrians, drones, and mobile RISs are agents. Figure 1 shows two types of RISs, namely reflective and transparent RISs. Both reflective and transparent RISs adjust the phase of scattered EM waves. The difference between reflective and transparent RISs is that signals pass through the transparent surfaces instead of being scattered [9]. Reflective and transparent RISs are deployed for different scenarios even though their principles are similar.

***HOLOGRAPHIC NLN IS A NEW PARADIGM FOR CONTROLLING THE EM ENVIRONMENT TO PROVIDE LOCATION AWARENESS IN CHALLENGING ENVIRONMENTS.***

Specifically, reflective RISs are deployed on the walls of buildings, whereas transparent RISs are used for the windows of the buildings. Both of these RISs create controlled connections between agents and anchors that allow wireless measurements and position information exchange that otherwise would be impossible due to the inadequacy of channels. For example, in Figure 1, the LOS path between the pedestrian on the left and Base Station 1 on Building A is obstructed by Building A and trees. Even though signals transmitted by Base Station 1 cannot reach the pedestrian via the LOS path, they can be received via the scattered paths created by RISs on the walls of Building B. This shows the capability of holographic NLN to employ spatial cooperation for improving the localization performance.

Moreover, an RIS can be viewed as an extended aperture for the receiver antenna and can improve the SNR at the receivers by intelligently adapting its phase response to direct the scattered signals toward the receiver. For example, the vehicle in Figure 1 is further away from Base Station 1 on Building A, and thus, the strength of the signal received by the vehicle via its LOS path to the Base Station 1 is low. To improve the SNR of the received signals, RISs on the walls of Building B can adjust their phase responses so that the scattered signals will be superimposed coherently at the vehicle. As a result, the vehicle can extract more position information from the measurements performed with the anchor and improve its localization accuracy.

Employing RISs to bridge indoor and outdoor environments for NLN is an example scenario for the deployment of transparent RISs. Many indoor localization techniques do not employ outdoor infrastructures as signals from these infrastructures are attenuated significantly when passing through walls. Wireless signals can propagate from an outdoor environment to an indoor environment via transparent RISs without suffering significant loss. In fact, the signals received by indoor nodes can even be intensified by carefully controlling the phase response

**A CONTROLLED EM ENVIRONMENT IS CREATED BY SENSING THE WIRELESS ENVIRONMENT AND ADJUSTING THE PHASE RESPONSES OF THE RISs ACCORDINGLY.**

of the transparent RISs. For example, signals transmitted by the outdoor Base Station 1 in Figure 1 can reach the inside of Building B via its transparent RISs without significant path loss. Such signals can be exploited by a user inside Building B to obtain position information.

Another benefit of RISs is that they can improve spatiotemporal cooperation in NLN. As a mobile agent equipped with RISs navigates through Building C, it can perform wireless measurements (e.g., range and relative angle) with different anchors and agents and extract position information from these measurements. Meanwhile, by communicating with different nodes, this mobile agent also creates a large network from what would otherwise be disconnected components. With such a network, the sensing, communication, and computing capabilities of different nodes can be employed collectively to obtain accurate position information. Note that RISs can be deployed on mobile devices whose primary objectives are neither communication nor localization (e.g., robots and vehicles). Since the RISs are lightweight, the power consumption incurred to mobilize these RISs is insignificant. Efficient deployment and configuration of RISs for holographic NLN can be obtained using estimation theory, optimization theory, and artificial intelligence techniques.

### *Characteristics of RISs for Holographic NLN*

#### Controllable Phase Response

The phase of a scattered EM wave can be controlled by RISs in real time and in a flexible manner. Consequently, RISs can significantly outperform electric scattering planes, for which the phases of the impinging signals are not controlled.

#### Large Aperture

The large aperture of an RIS enhances the robustness and performance of holographic NLN. The large aperture enables the localization system to combat the deterioration caused by undesirable and uncontrollable obstructions.

#### Additional Gain of High Operating Frequency

With an appropriate phase design, a high operating frequency can bring higher position information intensity for agents. This is because with the controlled phase response, more energy of the scattered wave can be directed toward the main lobe of the pattern of illuminated RIS as the operating frequency increases.

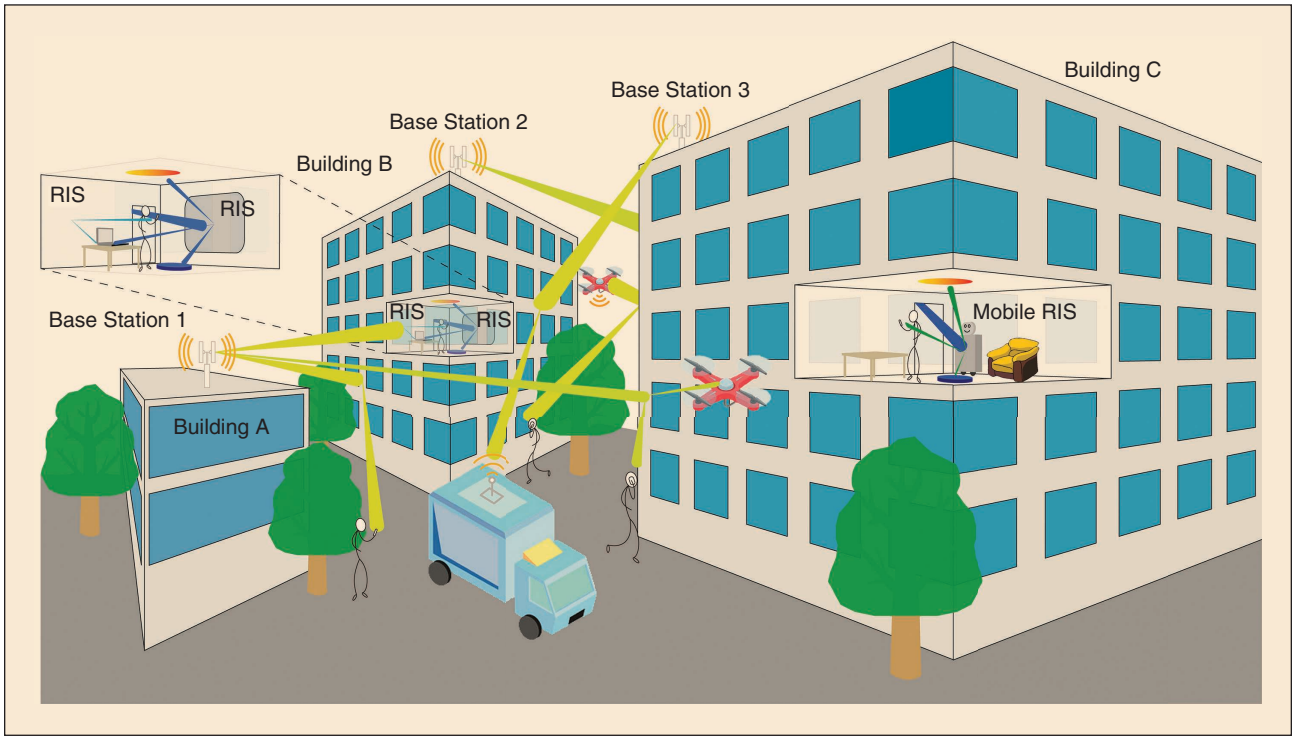


**FIGURE 1** An example of a scenario using holographic NLN. Blue square windows are transparent RISs, and gray patches on the walls are reflective RISs. RISs are used to improve localization and communication for vehicles, pedestrians, and indoor users.

### Mitigation of Signal Dispersion

In wideband systems, the frequency selectivity of wireless channels can lead to chromatic dispersion and thus degrade the system performance. In these scenarios, an RIS can be employed to combat the frequency selectivity of channels by optimizing the phase response of the RIS over the entire frequency band so that the signal scattered by the surface at different frequencies superimposes coherently at the receiver.

### Compatibility With Existing Systems and High Mobility

RISs are compatible with existing localization systems, and thus, holographic NLN can be implemented by only modifying the software to incorporate the cooperation between nodes and RISs. Moreover, RISs are typically lightweight and thus have high mobility.

## Models for ISs

Consider a localization system with an RIS, where an agent transmits signals to multiple anchors. The received signal at a particular anchor is

$$\mathbf{r}(t)=\begin{cases} r^{\mathrm{s}}(t)+r^{\mathrm{d}}(t)+\mathbf{n}(t), & \text{LOS} \\ r^{\mathrm{s}}(t)+\mathbf{n}(t), & \text{NLOS} \end{cases} \tag{1}$$

for any $t$ within an observation interval $[0, T_{\mathrm{obs}})$. Here, $r^{\mathrm{s}}(t)$ is the signal scattered by the agent-illuminated RIS, $r^{\mathrm{d}}(t)$ is the signal radiated from the agent, and $\mathbf{n}(t)$ is modeled as complex white Gaussian noise with the one-sided power spectral density of $N_0$. Equation (1) indicates that if the agent and the anchor are not in LOS, then no signal propagates from the agent to the anchor via the direct path.

RISs are continuous surfaces with controllable elements. Ideally, all points on the RISs can be controlled, as shown in Figure 2(a). An all-point-controllable RIS is referred to as a CIS. Its phase response is a continuous 2D function of each point of the surface. In practical systems, DISs whose elements are densely arranged on the surfaces [see Figure 2(b)], such as those with the spacing of elements set to half of the operating wavelength, can be viewed as an approximation of CISs. From a mathematical point of view, a DIS is a special case of CIS whose phase-response function is piece-wise constant. CISs can also serve as benchmarks when evaluating the effects of element size on the localization and communication performance. In the following, CISs and DISs are modeled accounting for the polarization of EM waves and the pattern of antennas.

The received signal component scattered by a CIS at the anchor is given by

$$r^{\mathrm{s}}(t)=\frac{\jmath k_0\sqrt{P}}{4\pi\sqrt{2R_{\mathrm{L}}}}\int_{\mathcal{S}}\gamma(\boldsymbol{q})F(\boldsymbol{q})\frac{e^{-\jmath k_0(l_{\mathrm{T}}(\boldsymbol{q})+l_{\mathrm{R}}(\boldsymbol{q}))}}{l_{\mathrm{T}}(\boldsymbol{q})l_{\mathrm{R}}(\boldsymbol{q})}e^{\jmath\Phi(\boldsymbol{q})}d\boldsymbol{q}, \tag{2}$$

where $\mathcal{S}$ is the set of all points of the RIS and $\boldsymbol{q}$ is the 2D coordinate of a point on the RIS on the $xy$-plane; $\Phi(\boldsymbol{q})$ is the controlled phase at point $\boldsymbol{q}$; $P$ is the transmitting power of the antenna of the agent; $R_{\mathrm{L}}$ is the radiation resistance of the antenna of the anchor; $\gamma(\boldsymbol{q})$ is the loss due to the polarization difference of the antenna at the anchor and the transmitted EM wave via the scattering path; $F(\boldsymbol{q})$ is the directive gain of the antennas of the anchors and the agent on the scattering path; $l_{\mathrm{T}}(\boldsymbol{q})$ is the distance between the agent and point $\boldsymbol{q}$ on the CIS; and $l_{\mathrm{R}}(\boldsymbol{q})$ is the distance between the point $\boldsymbol{q}$ on the CIS and the anchor, respectively. $k_0$ and $f_c$ are the vacuum wavenumber and the signal frequency, respectively. In addition, $\jmath$ is the imaginary unit.

**CISs and DISs are modeled accounting for the polarization of EM waves and the pattern of antennas.**

For comparison, the signal component $r^{\mathrm{s}}(t)$ scattered by an agent-illuminated DIS with $M\times N$ elements and received by the anchor is given by

$$r^{\mathrm{s}}(t)=\frac{\jmath k_0\sqrt{P}\zeta}{4\pi\sqrt{2R_{\mathrm{L}}}}\sum_{m=1}^{M}\sum_{n=1}^{N}\gamma(\boldsymbol{q}_{mn})F(\boldsymbol{q}_{mn}) \times\frac{e^{-\jmath k_0(l_{\mathrm{T}}(\boldsymbol{q}_{mn})+l_{\mathrm{R}}(\boldsymbol{q}_{mn}))}}{l_{\mathrm{T}}(\boldsymbol{q}_{mn})l_{\mathrm{R}}(\boldsymbol{q}_{mn})}e^{\jmath\Phi(\boldsymbol{q}_{mn})}, \tag{3}$$

where $\zeta$ is the area of the DIS element, and $\boldsymbol{q}_{mn}$ is the 2D coordinate of the $(m,n)$ element of the DIS on the $xy$-plane. Equation (3) is based on (2) and derived by using the Lagrange mean value theorem. It is worth noting that the signal model for DIS proposed in [15] for far-field scenarios can be viewed as a simplified form of (3) with the far-field assumption and with the influence of the polarization and directivity of antennas omitted.

CISs perform better beamforming than DIS as they can direct the scattered signal to the desired orientation by controlling the phase of every point on the surface.

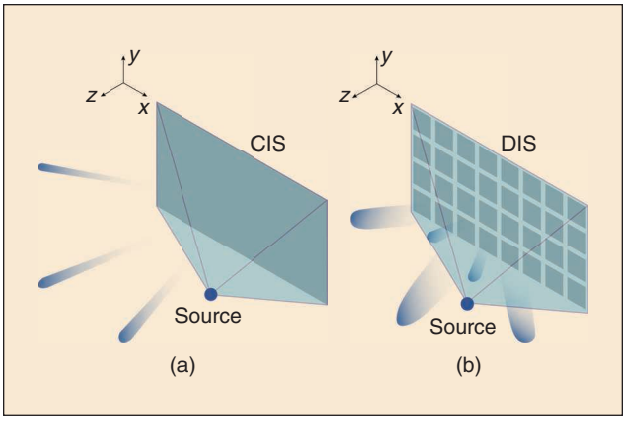


**FIGURE 2** Illustrations of (a) a CIS and (b) a DIS. The CIS provides a control on the phase, and thus, an improved beamforming compared to the DIS.

***Numerical results showed that with the aid of an RIS, the robustness of holographic localization to obstructions is significantly improved.***

For example, Figure 3 shows the normalized power of received signal scattered by a CIS and by different DISs consisting of square elements. The sizes of the CIS and DISs are all 3 m × 3 m, and multiple values of the length of each element for the DIS are considered. The phases of all the points on the CIS are designed to direct the scattered signals along the direction of 60° in the *yz*-plane, whereas the phase of each element for a DIS is set to that of the point on the CIS corresponding to the center of this element.

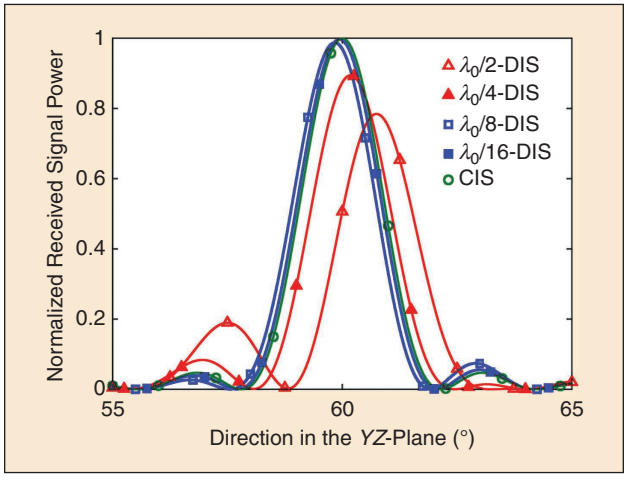


***Figure 3*** Normalized received signal power with respect to the direction of the receiver for a CIS and DISs with different element sizes.

Figure 3 shows that the CIS achieves 2.96 and 0.59 dB gain along the desired direction compared to DISs with $\lambda_0/2$ and $\lambda_0/4$ spacing, respectively. By contrast, the received power scattered by DISs deviates from the desired direction, and significant power is leaked into side lobes. Such performance degradation is more significant if a larger element length is adopted and thus the total number of elements decreases.

Figure 3 shows that DISs with element spacing below a quarter wavelength are close to CIS. Therefore, such DISs can be viewed as approximations for CISs in practical systems. Moreover, DISs with small element spacing (e.g., one-third wavelength) can be fabricated using printed circuit board techniques and thus would incur low hardware costs [13]. We envision that CISs can be employed as a cost-efficient solution for improving the accuracy, flexibility, and robustness of localization systems in the future.

## Case Study: Holographic Localization

### *Scenario*

Consider a localization system with one agent, three anchors, and a CIS (see Figure 4). The agent transmits signals to the anchors, and the received signals are used to infer the position of the agent. In this scenario, the agent does not perform any measurement, and all measurements are performed at the anchors. The agent can acquire its position knowledge by communicating with the anchors. Moreover, the CIS is obstructed by an obstacle, which blocks part of the EM waves scattered by the CIS. Specifically, the obstacle is modeled as a perfect

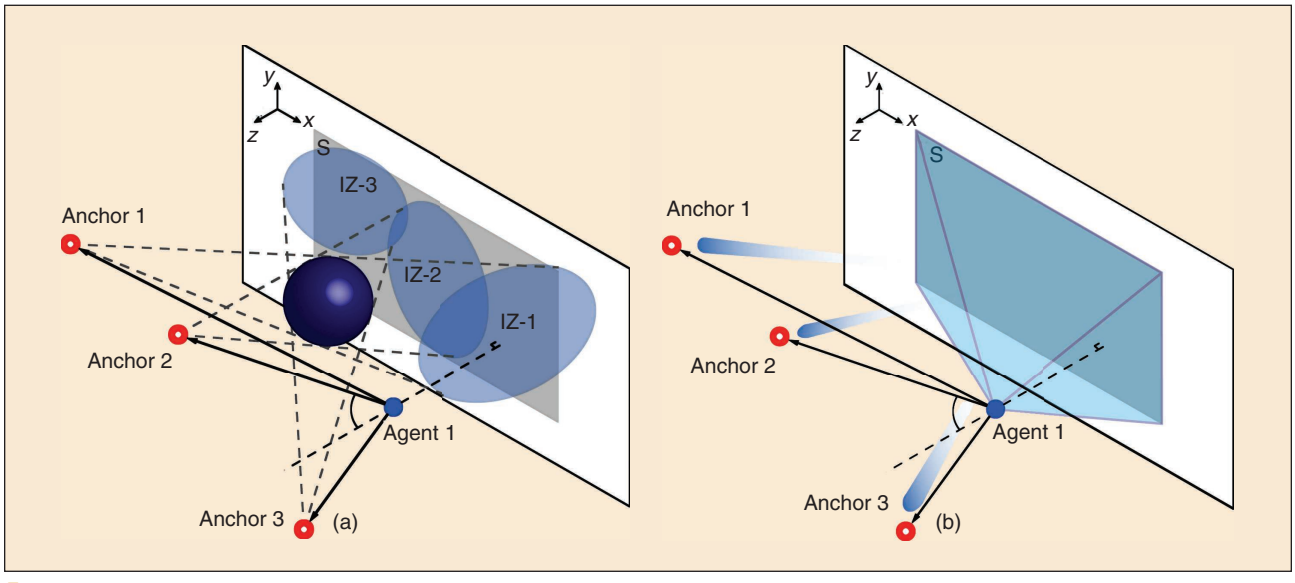


***Figure 4*** Illustrations of the case study with the described scenario and RIS advantages. (a) The scenario considered in the case study. (b) The benefit of an RIS for localization systems.

absorber, i.e., any signal that reaches the obstacle will be completely absorbed.

As a result, for each anchor, the signals scattered by part of the RIS in a certain region cannot be received. Such a region is referred to as the invalid zone (IZ) for that anchor. In particular, the IZ of an anchor is the shadow of the obstacle on the RIS for a virtual light source at that anchor. Moreover, the linear dimension of the obstacle is assumed to be significantly larger than the wavelength of the EM wave, and thus, diffraction can be ignored. Note that holographic NLN is not limited to scenarios where agents are transmitters and anchors are receivers. In general, agents can work as receivers and perform measurements.

The carrier frequency of the signals is 3 GHz, and half-operating-wavelength dipole antennas are adopted by both the agent and anchors. The transmitting power of the agent is 20 mW, the noise figure is 5 dB, and the duration of the signal is 66.67 μs. A 1 m × 1 m square CIS is deployed on the *xy*-plane of the coordinate system, and the center of the CIS coincides with the origin. The coordinates of anchors 1, 2, and 3 in a 3D space are (–220, 20, 300) (m), (–180, 18, 275) (m), and (–150, 15, 250) (m), respectively. The agent is placed randomly in a cubic region with coordinates given by [65, 70] (m) × [15, 25] (m) × [290, 300] (m). The obstacle is assumed to be a ball, and the coordinate of its center is (–7.5, 0, 6) (m). The element size of the DIS is half of the operating wavelength. Moreover, the step size for performing numerical 2D integrations over the RIS is 0.02 (m) × 0.02 (m).

Two configurations for the phase response of the RIS are considered in the simulation. In Configuration 1, IZs are not considered, and the phase response is designed such that signals scattered by all points on the RIS superimpose coherently at anchor 1. In Configuration 2, the phase response is designed with the IZ of each anchor accounted for. In particular, the phase response is designed such that the signals scattered by points not in IZ-1 superimpose coherently at anchor 1, the signals scattered by points in IZ-1 but not IZ-2 superimpose coherently at anchor 2, and the signals scattered by points in both IZ-1 and IZ-2 superimpose coherently at anchor 3. The RIS configurations can be achieved in practical systems with an iterative method: 1) perform rough estimation of the agent position with a randomly configured RIS and 2) refine the estimation by configuring RIS based on the rough estimation. Since the phase-response function of RISs can be expressed in a closed form, the complexity of each iteration is low. Furthermore, if prior knowledge of the agent position is available, the rough estimation can have sufficient accuracy, thus reducing the required number of iterations and the computational complexity for configuring the RISs.

***We envision that the employment of RISs can enhance the key features of NLN, such as spatiotemporal cooperation, efficient network operation, and soft information exploitation.***

### *Performance Evaluation*

Consider six cases with different setups of obstacles and phase-response configurations. Specifically, the obstacle on the scattering path (OSP) is absent in cases C1 and C2, and it is present in cases C3–C6. In cases C1, C3, and C5, the direct path between the agent and anchor 1 is completely obstructed by the obstacle on the direct path (ODP), whereas in cases C2, C4, and C6, there is a direct path between the agent and each anchor. Moreover, Configuration 1 is used for the phase response of the RIS in cases C1–C4, whereas Configuration 2 is used for cases C5 and C6. Details of each configuration are presented in the caption of Figure 5.

We evaluate the root squared position error bound (SPEB), which is a lower bound on localization uncertainty [6]. Specifically, the root SPEB of the agent is given by the root trace of the EFIM for the position of the agent. A smaller SPEB indicates that higher localization accuracy can be achieved.

Figure 5(a) shows the empirical cumulative distribution function (CDF) of the root SPEB for six cases when the radius of the obstacle $R_o$ is 2.7 m. In particular, the root SPEBs in cases C3 and C4 are larger than those in cases C1 and C2, respectively, as the RIS is partially obstructed by the obstacle and can provide lower performance gain. Moreover, the root SPEBs in cases C1 and C3 are larger than those in cases C2 and C4, respectively, since the signal can reach anchor 1 only via the scatter of the RIS.

Figure 5(a) also shows that better localization performance is achieved in cases C5 and C6 compared to cases C3 and C4, taken with Configuration 2 of the phase response. With this configuration, the beam formed by the points in IZ-1 is redirected to a different anchor. Therefore, the points in IZ-1 can increase the SNR of anchor 2 or anchor 3 and thus improve the localization performance. By contrast, with Configuration 1, signals scattered by points in IZ-1 superimpose incoherently at anchor 2 as well as anchor 3, and their contribution to the localization performance is insignificant. Therefore, as the size of the obstacle increases, the localization performance degrades.

Figure 5(b) shows the average root SPEB with respect to the radius of the obstacle for each of the six cases. Figure 5(b) shows two rows of percentage numbers beside the vertical dashed lines above the abscissa of the figure. Specifically, the numbers in the first and second

rows represent the maximum ratios and the average ratios, respectively, between the sizes of IZ-1, IZ-2, and IZ-3 and that of the RIS. Figure 5(b) shows that centimeter-level localization accuracy, in terms of root SPEB, can be achieved in all cases except case C3.

Moreover, the following two observations can be obtained from Figure 5(b). First, by carefully controlling the phase response of the RIS, decimeter-level localization accuracy can be achieved even in case C5 for large $R_o$, where both the direct path from the agent and the scattering paths from the RIS to anchor 1 are completely obstructed. Second, the average root SPEB in case C1, where a direct path is obstructed, is smaller than that in cases C4 and C6. This shows that the signals scattered by an unobstructed RIS can compensate for the loss of a direct path. These two observations demonstrate that holographic NLN is robust to obstructions by creating coherent superpositions of scattered signals at receivers.

Figure 5(a) and (b) compare the localization performance of DIS-enabled and CIS-enabled holographic NLN. In particular, the average root SPEBs of CIS-enabled holographic NLN are smaller than those of DIS-enabled holographic NLN in all six cases. Moreover, the performance of CIS-enabled holographic NLN with an ODP (solid line, C1) is better than that of DIS-enabled holographic NLN without any obstacle (dashed line, C2). Figure 5(a) also shows that the performance difference between DIS and CIS is more significant when the direct path is obstructed, indicating that CISs are more robust than DISs to NLOS conditions.

Results in this section show that, with the appropriate phase control, CIS can perform desirable beamforming by directing the scattered signal toward the direction of the anchors. Thanks to the large aperture of the CIS, the power of the received scattered signal is sufficiently large even though the signals suffer from stronger path loss compared to the signals received via the direct path, as illustrated in Figure 4(b). In addition, CIS creates scattered paths from the agent to anchors via phase control. These paths enable the communication between the agent and anchors even in the presence of an obstacle whose size is significantly larger than that of the CIS. The case study in this section can be extended to localization with multiple RISs. The performance gain brought by additional RISs depends on their positions, orientations, and sizes. Optimal configuration of multiple RISs requires cooperation among the RISs to control the wireless environment.

## Conclusion

This article introduced the paradigm of holographic NLN. In particular, RISs are employed in holographic NLN for creating an EM environment that is beneficial to localization. Favorable characteristics of RISs for NLN include their controllable phase responses, large apertures, and additional gain of high operating frequency as well as their capabilities to mitigate signal dispersion and

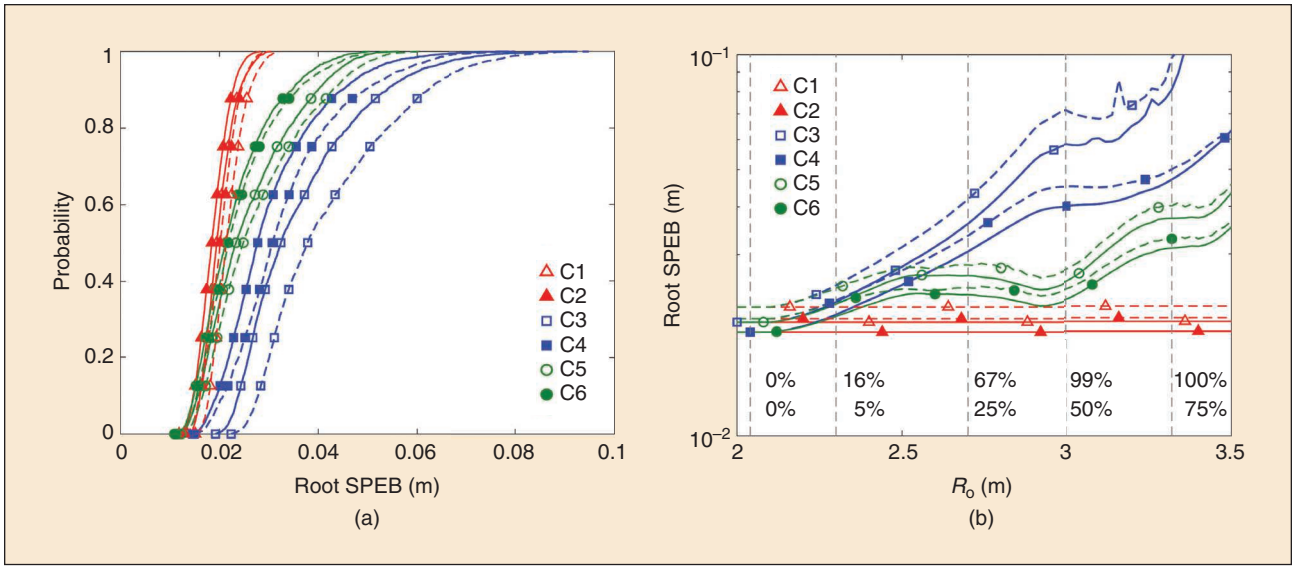


**FIGURE 5** The localization performance of the case studies. Dashed lines denote the results of the DIS, and solid lines denote the results of the CIS. Six cases are considered in a localization system with one agent, three anchors, and an RIS. (a) The empirical CDF of root SPEB for $R_o$ = 2.7 m. (b) The average root SPEB with respect to the radius $R_o$ of the obstacle. C1: ODP + Configuration 1 RIS; C2: Configuration 1 RIS; C3: OSP + ODP + Configuration 1 RIS; C4: OSP + Configuration 1 RIS; C5: OSP + ODP + Configuration 2 RIS; C6: OSP + Configuration 2 RIS.

improve the mobility of localization systems. We first briefly reviewed RISs and presented the concepts of CIS and DIS. Then, we provided signal models for CIS and DIS, accounting for polarization and the patterns of antennas, and showed that the model for DIS can be viewed as a special case of that of CIS and that the phase response of CISs can be better controlled compared to that of DISs. Finally, a case study is presented for the performance of a holographic localization system in the presence of obstructions. Numerical results showed that with the aid of an RIS, the robustness of holographic localization to obstructions is significantly improved. We envision that the employment of RISs can enhance the key features of NLN, such as spatio-temporal cooperation, efficient network operation, and soft information exploitation for high-accuracy LBSs. Holographic NLN enabled by RISs paves the way to a new level of location awareness.

## Acknowledgments

The fundamental research described in this article was supported, in part, by the Office of Naval Research under Grants N00014-16-1-2141 and N62909-22-1-2009, the European Union's Horizon 2020 Research and Innovation Programme under Grant 871249, and the Massachusetts Institute of Technology Institute for Soldier Nanotechnologies.

## Author Information

***Moe Z. Win*** (moewin@mit.edu) is a professor with the Laboratory for Information and Decision Systems, Massachusetts Institute of Technology, Cambridge, Massachusetts, 02139-4307, USA. His research interests include network localization and navigation, network interference exploitation, and quantum information science. He is a Fellow of IEEE.

***Ziyi Wang*** (ziyiwang@mit.edu) is a graduate student with the Wireless Information and Network Sciences Laboratory, Massachusetts Institute of Technology, Cambridge, Massachusetts, 02139-4307, USA. His research interests include wireless communication, network localization and navigation, and reconfigurable intelligent surfaces. He is a Graduate Student Member of IEEE.

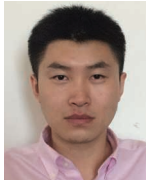

***Zhenyu Liu*** (zliu14@mit.edu) is a graduate student with the Wireless Information and Network Sciences Laboratory, Massachusetts Institute of Technology, Cambridge, Massachusetts, 02139-4307, USA. His research interests include wireless communications, network localization, distributed inference, stochastic optimization, and networked control. He is a Graduate Student Member of IEEE.

***Yuan Shen*** (shenyuan_ee@tsinghua.edu.cn) is a professor with the Department of Electronic Engineering at Tsinghua University, Beijing, 100084, China. His research interests include network localization and navigation, integrated sensing and communication, and multiagent systems. He is a Senior Member of IEEE.

***Andrea Conti*** (a.conti@ieee.org) is a professor with the Department of Engineering and Consorzio Nazionale Interuniversitario per le Telecomunicazioni, University of Ferrara, Ferrara, 44122, Italy. His research topics include network localization and navigation, distributed sensing, adaptive diversity communications, and quantum information science. He is a Fellow of IEEE.

## References

[1] M. Z. Win *et al.*, "Network localization and navigation via cooperation," *IEEE Commun. Mag.*, vol. 49, no. 5, pp. 56–62, May 2011, doi: 10.1109/MCOM.2011.5762798.

[2] J. Zhang, H. Du, Q. Sun, B. Ai, and D. W. K. Ng, "Physical layer security enhancement with reconfigurable intelligent surface-aided networks," *IEEE Trans. Inf. Forensics Security*, vol. 16, pp. 3480–3495, May 2021, doi: 10.1109/TIFS.2021.3083409.

[3] C. Pan, H. Ren, K. Wang, W. Xu, M. Elkashlan, A. Nallanathan, and L. Hanzo, "Multicell MIMO communications relying on intelligent reflecting surfaces," *IEEE Trans. Wireless Commun.*, vol. 19, no. 8, pp. 5218–5233, 2020, doi: 10.1109/TWC.2020.2990766.

[4] X. Chen *et al.*, "Design and implementation of MIMO transmission based on dual-polarized reconfigurable intelligent surface," *IEEE Wireless Commun. Lett.*, vol. 10, no. 10, pp. 2155–2159, 2021, doi: 10.1109/LWC.2021.3095172.

[5] A. Elzanaty, A. Guerra, F. Guidi, D. Dardari, and M.-S. Alouini, "Towards 6G holographic localization: Enabling technologies and perspectives," 2021, *arXiv:2103.12415*.

[6] M. Z. Win, Y. Shen, and W. Dai, "A theoretical foundation of network localization and navigation," *Proc. IEEE*, vol. 106, no. 7, pp. 1136–1165, Jul. 2018, doi: 10.1109/JPROC.2018.2844553.

[7] M. D. Renzo *et al.*, "Smart radio environments empowered by reconfigurable intelligent surfaces: How it works, state of research, and the road ahead," *IEEE J. Sel. Areas Commun.*, vol. 38, no. 11, pp. 2450–2525, Jul. 2020, doi: 10.1109/JSAC.2020.3007211.

[8] C. Huang *et al.*, "Holographic MIMO surfaces for 6G wireless networks: Opportunities, challenges, and trends," *IEEE Wireless Commun.*, vol. 27, no. 5, pp. 118–125, Oct. 2020, doi: 10.1109/MWC.001.1900534.

[9] O. Tsilipakos *et al.*, "Toward intelligent metasurfaces: The progress from globally tunable metasurfaces to software-defined metasurfaces with an embedded network of controllers," *Adv. Opt. Mater.*, vol. 8, no. 17, p. 2,000,783, 2020, doi: 10.1002/adom.202000783.

[10] N. Yu *et al.*, "Light propagation with phase discontinuities: Generalized laws of reflection and refraction," *Science*, vol. 334, no. 6054, pp. 333–337, Oct. 2011, doi: 10.1126/science.1210713.

[11] S. Sun, Q. He, S. Xiao, Q. Xu, X. Li, and L. Zhou, "Gradient-index metasurfaces as a bridge linking propagating waves and surface waves," *Nature Mater.*, vol. 11, no. 5, pp. 426–431, May 2012, doi: 10.1038/nmat3292.

[12] T. J. Cui, M. Q. Qi, X. Wan, J. Zhao, and Q. Cheng, "Coding metamaterials, digital metamaterials and programmable metamaterials," *Light: Sci. Appl.*, vol. 3, no. 10, pp. e218–e218, Oct. 2014, doi: 10.1038/lsa.2014.99.

[13] O. Yurduseven, D. L. Marks, T. Fromenteze, and D. R. Smith, "Dynamically reconfigurable holographic metasurface aperture for a Mills-Cross monochromatic microwave camera," *Opt. Exp.*, vol. 26, no. 5, pp. 5281–5291, Mar. 2018, doi: 10.1364/OE.26.005281.

[14] A. Conti, S. Mazuelas, S. Bartoletti, W. C. Lindsey, and M. Z. Win, "Soft information for localization-of-things," *Proc. IEEE*, vol. 107, no. 11, pp. 2240–2264, Nov. 2019, doi: 10.1109/JPROC.2019.2905854.

[15] Q. Wu and R. Zhang, "Intelligent reflecting surface enhanced wireless network via joint active and passive beamforming," *IEEE Trans. Wireless Commun.*, vol. 18, no. 11, pp. 5394–5409, Nov. 2019, doi: 10.1109/TWC.2019.2936025.

***VT***